Experimental Determination of In-Medium Cluster Binding Energies and Mott Points in Nuclear Matter

K. Hagel,[1] R. Wada,[2,1] L. Qin,[1] J. B. Natowitz,[1] S. Shlomo,[1] A. Bonasera,[1,3] G. Röpke,[4] S. Typel,[5] Z. Chen,[2] M. Huang,[2] J. Wang,[2] H. Zheng,[1] S. Kowalski,[6] C. Bottosso,[1] M. Barbui,[1] M. R. D. Rodrigues,[1] K. Schmidt,[1] D. Fabris,[7] M. Lunardon,[7] S. Moretto,[7] G. Nebbia,[7] S. Pesente,[7] V. Rizzi,[7] G. Viesti,[7] M. Cinausero,[8] G. Prete,[8] T. Keutgen,[9] Y. El Masri,[9] and Z. Majka[10]

[1]*Cyclotron Institute, Texas A&M University, College Station, Texas 77843, USA*
[2]*Institute of Modern Physics HIRFL, Chinese Academy of Sciences, Lanzhou, 730000, China*
[3]*Laboratori Nazionali del Sud, INFN, via Santa Sofia, 62, 95123 Catania, Italy*
[4]*University of Rostock, FB Physik, Rostock, Germany*
[5]*GSI Helmholtzzentrum für Schwerionenforschung GmbH, Theorie, Planckstraße 1, D-64291 Darmstadt, Germany*
[6]*Institute of Physics, Silesia University, Katowice, Poland*
[7]*Dipartamento di Fisica dell Universita di Padova and INFN Sezione di Padova, Padova, Italy*
[8]*INFN Laboratori Nazionali di Legnaro, Legnaro, Italy*
[9]*FNRS and IPN, Université Catholique de Louvain, B-1348 Louvain-Neuve, Belgium*
[10]*Smoluchowski Institute of Physics, Jagiellonian University, Krakow, Poland*
(Received 15 November 2011; published 10 February 2012)

In-medium binding energies and Mott points for d, t, ^{3}He and α clusters in low-density nuclear matter have been determined at specific combinations of temperature and density in low-density nuclear matter produced in collisions of 47A MeV ^{40}Ar and ^{64}Zn projectiles with ^{112}Sn and ^{124}Sn target nuclei. The experimentally derived values of the in-medium modified binding energies are in good agreement with recent theoretical predictions based upon the implementation of Pauli blocking effects in a quantum statistical approach.

DOI: 10.1103/PhysRevLett.108.062702 PACS numbers: 25.70.Pq

I. Introduction.—Simple nuclear statistical equilibrium models assume that the properties of the species in equilibrium are the same as those of the isolated species. While this assumption is tenable at very low density, it is untenable at higher densities where in-medium effects lead to dissolution of the clusters and a transition to cluster-free nuclear matter. To deal with this intermediate density range, Typel *et al.* [1] have developed a quantum statistical approach which includes cluster correlations in the medium and interpolates between the exact low-density limit and the very successful relativistic mean field (RMF) approaches appropriate near the saturation density. The generalized RMF model developed attributes the decrease of the cluster fractions at high densities to a reduction of the cluster binding energies due to the Pauli blocking. This leads to the Mott effect of vanishing binding [2]. Well-defined clusters appear only for densities below approximately $1/10$ of the saturation density and get dissolved at higher densities. The maximum cluster density is reached around the Mott density. Because of the presence of strong correlations in the scattering state continuum that are effectively represented by one resonance, there is a nonvanishing cluster fraction above the Mott density [3]. We report here the first experimental derivation of temperature and density dependent binding energies of d, t, ^{3}He and α clusters, directly from experimental particle yields. Experimental values for Mott points for d, t, ^{3}He and α clusters are in good agreement with the predictions made in Ref. [1].

II. Experimental techniques.—We reported in Refs. [4,5] that measurements of nucleon and light cluster emission from the participant matter which is produced in near Fermi energy heavy ion collisions could be employed to probe the EOS at low density and moderate temperatures where clustering is important. The NIMROD 4π multidetector at Texas A&M University has now been used to extend our measurements to higher densities. Cluster production in collisions of 47A MeV ^{40}Ar with ^{112,124}Sn and ^{64}Zn with ^{112,124}Sn was studied. NIMROD consists of a 166 segment charged particle array set inside a neutron ball [6]. The charged particle array is arranged in 12 rings of Si-CsI telescopes or single CsI detectors concentric around the beam axis. The CsI detectors are 1–10 cm thick Tl doped crystals read by photomultiplier tubes. A pulse shape discrimination method is employed to identify light particles in the CsI detectors. Neutron multiplicity is measured with the 4π neutron detector surrounding the charged particle array. The combined neutron and charged particle multiplicities were employed to select the most violent events for subsequent analysis. Further details on the detection system, energy calibrations, and neutron ball efficiency may be found in Ref. [6].

III. Analysis.—The dynamics of the collision process allow us to probe the nature of the intermediate velocity

''nucleon-nucleon'' emission source [7–10]. Measurement of emission cross sections of nucleons and light clusters together with suitable application of a coalescence ansatz [7] provides the means to probe the properties and evolution of the interaction region. The techniques used have been detailed in several previous publications [4,5,8–11] and are described briefly below. A notable difference from Refs. [4,5] is the method of density extraction. This is discussed more extensively in the following. We emphasize that the event selection is on the more violent collisions. Cross section weighting favors midrange impact parameters.

An initial estimation of emission multiplicities at each stage of the reaction was made by fitting the observed light particle spectra assuming contributions from three sources, a projectilelike fragment (PLF) source, an intermediate velocity (IV) source, and a targetlike fragment (TLF) source. A reasonable reproduction of the observed spectra is achieved. Except for the most forward detector rings the data are dominated by particles associated with the IV and TLF sources. The IV source velocities are very close to 50% of the beam velocity as seen in many other studies ([7–10] and references therein). The observed spectral slopes reflect the evolution dynamics of the source [10,12,13]. For further analysis, this IV source is most easily sampled at the intermediate angles where contributions from the other sources are minimized. For the analysis of the evolution of the source we have selected the data in ring 9 of the NIMROD detector. This ring covered an angular range in the laboratory of 38° to 52°. The results of the three-source fit analyses, as well as inspection of invariant velocity plots constructed for each ejectile and each system, indicate that this selection of angular range minimizes contributions from secondary evaporative decay of projectilelike or targetlike sources [11].

We treat the IV source as a nascent fireball created in the participant interaction zone. The expansion and cooling of this zone leads to a correlated evolution of density and temperature which we probe using particle and cluster observables, yield, energy, and angle. As in the previous work [4,5] we have employed double isotope yield ratios [14,15] to characterize the temperature at a particular emission time. Model studies comparing Albergo model temperatures and densities to the known input values have shown the double isotope ratio temperatures to be relatively robust in this density range [16]. However, the densities extracted using the Albergo model are useful only at the very lowest densities [16]. Both of these results are confirmed in the more extensive calculations of Ref. [1]. In this study we have employed a different means of density extraction, the thermal coalescence model of Mekjian [8,10].

To determine the coalescence parameter P_0, the radius in momentum space, from our data we have followed the Coulomb-corrected coalescence model formalism of Awes *et al.* [17] and previously employed by us in Ref. [7]. In the laboratory frame the derived relationship between the observed cluster and proton differential cross sections is

$$\frac{d^2N(Z,N,E_A)}{dE_A d\Omega} = R_{np}^N \frac{A^{-1}}{N!Z!}\left(\frac{\frac{4}{3}\pi P_0^3}{[2m^3(E-E_C)]^{(1/2)}}\right)^{A-1} \times \left(\frac{d^2N(1,0,E)}{dEd\Omega}\right)^A, \quad (1)$$

where the double differential multiplicity for a cluster of mass number A containing Z protons and N neutrons and having a Coulomb-corrected energy E_A, is related to the proton double differential multiplicity at the same Coulomb-corrected energy per nucleon, $E - E_C$, where E_C is the Coulomb barrier for proton emission. R_{np} is the neutron to proton ratio. Since within the framework of the coalescence model the yield ratios of two isotopes which differ by one neutron are determined by their binding energies and the n/p ratio in the coalescence volume, we have used the observed triton to ^{3}He yield ratio to derive the n/p ratio used in this analysis.

In the Mekjian model thermal and chemical equilibrium determines coalescence yields of all species. Under these assumptions there is a direct relationship between the derived radius in momentum space and the volume of the emitting system. In terms of the P_0 derived from Eq. (1) and assuming a spherical source

$$V = \left[\left(\frac{Z!N!A^3}{2^A}\right)(2s+1)e^{\frac{E_0}{T}}\right]^{1/(A-1)} \frac{3h^3}{4\pi P_0^3} \quad (2)$$

where h is Planck's constant and Z, N, and A are the same as in Eq. (1), E_0 is the binding energy and s the spin of the emitted cluster and T is the temperature. Thus the volume can be derived from the observed P_0 and temperature values assuming a spherical shape in terms of the P_0 derived from Eq. (1).

Because our goal was to derive information on the density and temperature evolution of the emitting system, our analysis was not limited to determining an average P_0 value. Instead, as in our previous studies [4,5,8], results for d, t, ^{3}He, and ^{4}He, were derived as a function of $v_{\rm surf}$, the velocity of the emerging particle at the nuclear surface, prior to Coulomb acceleration [17]. From the relevant P_0 values we then determined volumes using Eq. (2). A comparison of these volumes indicated good agreement for t, ^{3}He and ^{4}He. The volumes derived from the deuteron data are typically somewhat smaller. This appears to reflect the fragility of the deuteron and its survival probability once formed [18]. For this reason we have used average volumes derived from the $A = 3$ and 4 clusters to calculate the densities. Given that mass is removed from the system during the evolution, we determined the relevant masses for each volume by assuming that the initial mass of the source was that determined from the source fitting analysis and then determining the mass remaining at a given $v_{\rm surf}$ from the observed energy spectra. This is also an averaging

process and ignores fluctuations. Densities were determined by dividing remaining masses by volumes.

IV. Results.—

A. Temperatures and densities.—Inspection of the results for the four different systems studied revealed that the temperatures, densities for all systems are the same within statistical uncertainties. Therefore we have combined them to determine the values reported in this Letter.

We present, in Fig. 1 the experimentally derived density and temperature evolution of the IV source. Estimated errors on the temperatures are 10% below $\rho = 0.01$ fm^{-3} increasing to 15% at $\rho = 0.03$ fm^{-3}. Estimated errors on the densities are 20%.

In a recently submitted paper we reported equilibrium constants for α cluster formation as a function of temperature and density [19]. These equilibrium constants were then compared with those predicted by several different astrophysical equation of state models. Specifically, we defined the equilibrium constants, K_c, for cluster formation in terms of density as

$$K_c(A, Z) = \rho_{(A,Z)}/[(\rho_p)^Z(\rho_n)^N], \quad (3)$$

where $\rho_{(A,Z)}$ is the density of clusters of a specific mass number A and atomic number Z, N is the neutron number in the cluster, and ρ_p and ρ_n are, respectively, the densities of free protons and neutrons. In the present work, we employ the observed temperature and density dependence of these equilibrium constants to extract the in-medium modifications of the cluster binding energies and determine Mott points.

V. Derivation of in-medium binding energies.—Our departure point for extraction of the medium modified cluster binding energies is the chemical equilibrium expression relating the density of a cluster of mass number A and atomic number Z to the densities of neutrons and protons in the same volume V [12].

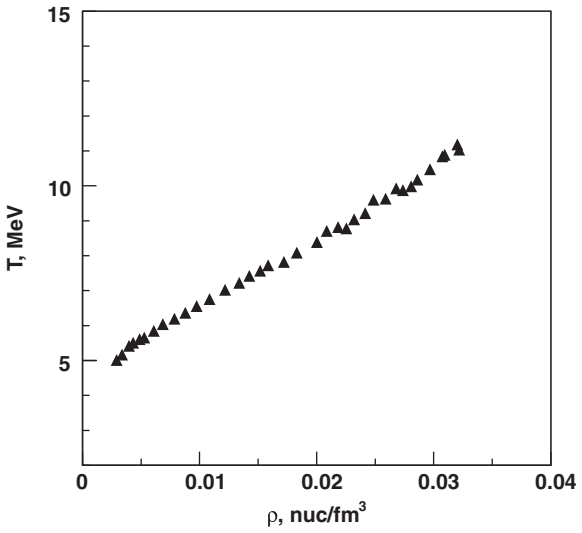

FIG. 1. Temperatures and densities sampled by the expanding IV source.

$$\rho(A, Z) = \frac{N(A, Z)}{V} = \frac{A^{3/2}\lambda_T^{3(A-1)}\omega(A, Z)}{(2s_p + 1)^Z(2s_n + 1)^{A-Z}} \times \rho_p^Z\rho_n^{A-Z}\exp\left(\frac{B(A, Z)}{T}\right). \quad (4)$$

In this expression, $\lambda_T = \frac{h}{(2\pi m_0 T)^{1/2}}$ is the thermal wavelength of a nucleon, s_p and s_n are the proton and neutron spins, T is the temperature, and $B(A, Z)$ is the cluster binding energy. The term $\omega(A, Z)$ is the internal partition function of the cluster, taken here to 1 for the $Z = 1$ and $Z = 2$ clusters considered.

Minich *et al.* [20,21] used a related yield expression to analyze intermediate mass fragment yields in multifragmentation experiments but added both a mixing entropy term and a surface entropy term, as initially proposed by Fisher [22]. This latter term leads to a power law behavior of the mass distribution at the critical point and its ramifications have been widely explored [23–25]. Neither of these entropy contributions is explicitly included in the Albergo formulation [12]. In the present analysis of the experimental data we include a mixing entropy term in the free energy. This term has the form

$$\Delta F = T(Z\ln(Z/A) + N\ln(N/A)), \quad (5)$$

where once again Z, N, and A are those of the cluster being formed [20]. As mixing is a spontaneous process the free energy of mixing is negative and therefore favors the cluster formation. We do not include a Fisher term. Our reasoning for this is that, without additional corrections, the Fisher term as normally formulated and applied to larger clusters whose properties are very similar to the bulk properties, is not applicable to the yields of the very small clusters, $A \leq 4$, which we are treating. We base this conclusion on the results of molecular dynamics studies of

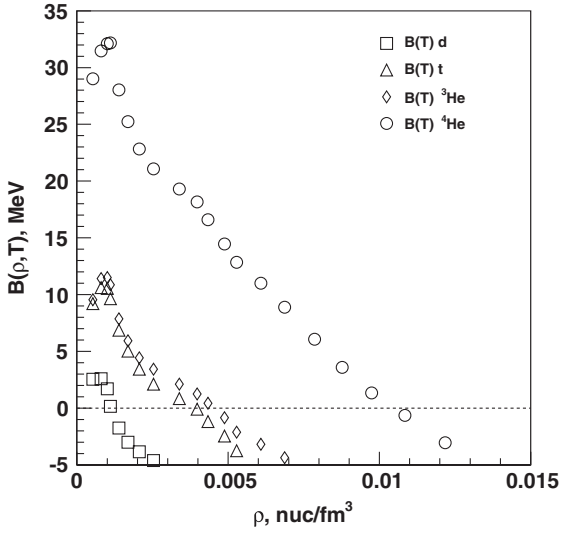

FIG. 2. In-medium binding energies derived from the experiments as a function of density. T and ρ are changing in a correlated fashion. (See text.)

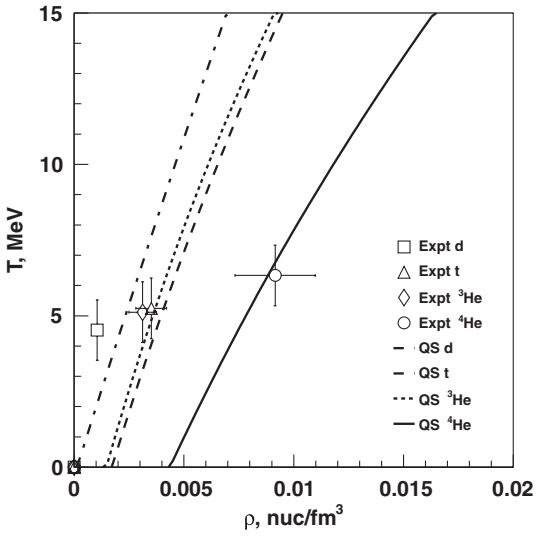

FIG. 3. Comparison of experimentally derived Mott point densities and temperatures with theoretical values. Symbols represent the experimental data. Estimated errors on the temperatures are 10% and on the densities 20%. Lines show polynomial fits to the Mott points presented in Ref. [1].

the cluster size dependence of the surface energy [26–28] and the binding energies per nucleon of the competing $Z = 1, 2$ species being significantly different from the bulk.

Thus, rearranging Eq. (4), substituting K_c from Eq. (3), and taking the logarithm of each side we can write a general expression for each cluster,

$$\ln[K_c/C(T)] = B/T - Z\ln(Z/A) - N\ln(N/A), \quad (6)$$

where $C(T)$ includes all terms on the right-hand side of Eq. (4) except the exponential term. Using the experimentally determined equilibrium constants and temperatures we then solve this expression to obtain the apparent binding energies, $B(\rho, T)$, of the clusters for the different temperatures and densities sampled in the experiments. The binding energies extracted for d, t, ^{3}He, and α clusters decrease monotonically with increasing density as shown in Fig. 2.

VI. Mott points.—By definition, a Mott point corresponds to a combination of density and temperature at which a cluster binding energy, $B(\rho, T)$, is zero with respect to the surrounding medium. Since the observed temperatures and densities are correlated in our experiment (see Fig. 1) each point in Fig. 2 at which the experimentally derived binding energy is zero corresponds to a particular combination of density and temperature. Thus, with the present data, we are able to extract a single Mott point for each cluster. In Fig. 3 we present the values of the Mott temperatures and densities and compare them with the loci of the values of medium modified binding energies predicted by Typel *et al.* [1] using the thermodynamic Green function method. Such a Mott line was also calculated in Ref. [29] while the contribution of correlations was considered without discriminating among different clusters. This approach makes explicit use of an effective nucleon-nucleon interaction to account for medium effects on the cluster properties [30]. We see that the agreement between the predictions and the experimental results is quite good.

VII. Summary and conclusions.—We have presented a first experimental determination of in-medium cluster binding energies and Mott points for d, t, ^{3}He and α clusters produced in low-density nuclear matter. Our results are in good agreement with those predicted by a recent model which explicitly treats these quantities. Inclusion of the in-medium effects in astrophysical equations of state should improve the utility of those for modeling astrophysically interesting events.

This work was supported by the United States Department of Energy under Grant No. DE-FG03-93ER40773 and by The Robert A. Welch Foundation under Grant No. A0330.

[1] S. Typel, G. Röpke, T. Klähn, D. Blaschke, and H. H. Wolter, Phys. Rev. C **81**, 015803 (2010).
[2] G. Röpke *et al.*, Nucl. Phys. A **379**, 536 (1982).
[3] M. Schmidt *et al.*, Ann. Phys. (N.Y.) **202**, 57 (1990).
[4] S. Kowalski *et al.*, Phys. Rev. C **75**, 014601 (2007).
[5] J. B. Natowitz *et al.* Phys. Rev. Lett. **104**, 202501 (2010).
[6] S. Wuenschel *et al.*, Nucl. Instrum. Methods Phys. Res., Sect. A **604**, 578 (2009).
[7] A. Z. Mekjian, Phys. Rev. C **17**, 1051 (1978); Phys. Rev. Lett. **38**, 640 (1977).
[8] K. Hagel *et al.*, Phys. Rev. C **62**, 034607 (2000).
[9] R. Wada *et al.*, Phys. Rev. C **39**, 497 (1989).
[10] R. Wada *et al.*, Phys. Rev. C **69**, 044610 (2004).
[11] L. Qin, thesis, Texas A&M University, 2008.
[12] S. Albergo *et al.*, Nuovo Cimento A **89**, 1 (1985).
[13] A. Kolomiets, V. M. Kolomietz, and S. Shlomo, Phys. Rev. C **55**, 1376 (1997).
[14] W. Bauer, Phys. Rev. C **51**, 803 (1995).
[15] H. Zheng *et al.*, Phys. Lett. B **696**, 178 (2011).
[16] S. Shlomo *et al.*, Phys. Rev. C **79**, 034604 (2009).
[17] T. C. Awes *et al.*, Phys. Rev. C **24**, 89 (1981).
[18] I. Cervesato *et al.*, Phys. Rev. C **45**, 2369 (1992).
[19] L. Qin *et al.*, arXiv:1110.3345 [Phys. Rev. Lett. (to be published)].
[20] R. W. Minich, *et al.*, Phys. Lett. B **118**, 458 (1982).
[21] A. S. Hirsch *et al.*, Nucl. Phys. **A418**, 267 (1984).
[22] M. E. Fisher, Physics, **3**, 225 (1967); Rep. Prog. Phys. **30**, 615 (1967).
[23] J. B. Elliott *et al.*, Phys. Rev. C **67**, 024609 (2003).
[24] J. B. Elliott *et al.*, Phys. Rev. Lett. **85**, 1194 (2000).
[25] M. Huang *et al.*, Phys. Rev. C **82**, 054602 (2010).
[26] B. Hale, Aust. J. Phys. **49**, 425 (1996) [http://www.publish.csiro.au/nid/78/paper/PH960425.htm].
[27] J. Kiefer and B. N. Hale, AIP Conf. Proc., **534**, 260 (2000).
[28] M. W. Curtin *et al.*, Phys. Lett. B **123**, 289 (1983).
[29] H. Stein *et al.*, Z. Phys. A **351**, 295 (1995).
[30] G. Röpke, *et al.*, Nucl. Phys. **A399**, 587 (1983).